Multielectron Transitions Induced by Neutron Impact on Helium

M. Liertzer, J. Feist, S. Nagele, and J. Burgdörfer

Phys. Rev. Lett. **109**, 013201 — Published 2 July 2012

DOI: 10.1103/PhysRevLett.109.013201

Multi-electron transitions induced by neutron impact on helium

M. Liertzer,[1,*] J. Feist,[2,1] S. Nagele,[1] and J. Burgdörfer[1]

[1] *Institute for Theoretical Physics, Vienna University of Technology, 1040 Vienna, Austria, EU*
[2] *ITAMP, Harvard-Smithsonian Center for Astrophysics, Cambridge, Massachusetts 02138, USA*

We explore excitation and ionization by neutron impact as a novel tool for the investigation of electron-electron correlations in helium. We present single and double ionization spectra calculated in accurate numerical ab-initio simulations for incoming neutrons with kinetic energies of up to 150 keV. The resulting electron spectra are found to be fundamentally different from photoionization or charged particle impact due to the intrinsic many-body character of the interaction. In particular, doubly excited resonances that are strongly suppressed in electron or photon impact become prominent. The ratio of double to single ionization is found to differ significantly from those of photon and charged particle impact.

PACS numbers: 34.80.Dp, 32.30.-r, 61.05.fg, 31.15.A-

A theme of central importance in atomic, molecular, and condensed matter physics is the understanding and description of electron-electron correlations. The simplest and most fundamental system featuring strong electron correlations is the helium atom [1]. For the last half a century it has served as the "Rosetta Stone" for correlated dynamics beyond the single-particle picture stimulating the development of a multitude of novel concepts ranging from many-body break-up laws [2] and Beutler-Fano resonances [3] to collective quantum numbers [4] and provided the testing ground for novel theoretical methods such as many-body perturbation theory [5] or hyperspherical-coordinate methods [6]. As the two-electron problem, both in stationary states as well as driven by external fields, can nowadays be treated exactly by numerical ab-initio calculations, it allows, in unprecedented detail, to explore dynamical correlations, when probed by charged particle or photon impact [7, 8]. The observables accessible by such probes are, however, limited by either exact selection rules or approximate "propensity" rules. For example, photoabsorption spectroscopy is strongly dominated by dipole-allowed transitions. In charged-particle impact, higher multipole transitions are allowed but are typically suppressed in "soft" collisions with small momentum transfers. Moreover, the long-range Coulomb interactions between the probing particle and the excited system may distort the excitation and ionization to be extracted by "post-collision" interactions which are typically beyond lowest-order perturbation (LOP) theory underlying linear response.

In this Letter we theoretically investigate neutron impact ionization as a further probing method for studying electron-electron correlations [9]. The underlying idea is that neutron scattering at the atomic nucleus gives rise to a sudden simultaneous momentum boost for *all* electrons, effectively causing a true *many-body* transition which can lead to multiple excitation and ionization of the atom. This is in contrast to photon and charged particle interactions where the LOP interaction is strictly a one-body operator. Using neutron impact ionization we can therefore directly probe the momenta of the electrons in the ground state of helium.We show that neutron impact leads to a very broad energy distribution in the final states including double ionization and, furthermore, that it can efficiently produce strongly correlated doubly excited resonances that are disfavored by other probing agents.

We assume that the only interaction in the neutron-helium collision is elastic scattering between the neutron and the nucleus, mediated by the strong nuclear force. The contributions of magnetic interactions of the neutron with the electronic and nuclear magnetic moment are small enough to be safely neglected [10]. Neutron energies are kept sufficiently low in order to exclude any inelastic nuclear processes. The duration of the neutron-nucleus scattering event is much shorter than the typical time scale of the dynamics of electrons bound to the nucleus ($\sim$ attoseconds) currently probed using ultrashort light pulses [11–13]. Electronic transitions can therefore be described by an impulse or "sudden" approximation. Accordingly, the transition amplitude for elastic scattering of the neutron accompanied by an electronic transition $i \to f$ is given by

$$t_{if}(\Delta\vec{p}_{nuc}) \approx t^{el}_{nuc}(\Delta\vec{p}_{nuc}) \cdot t^{e}_{i,f}(\Delta\vec{p}_{e}), \qquad (1)$$

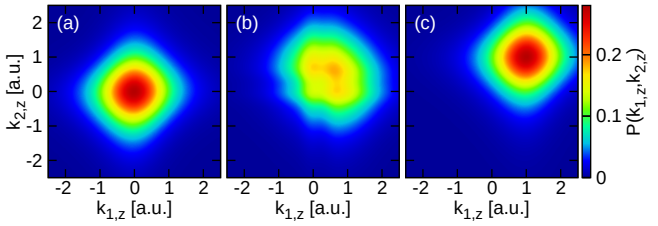

FIG. 1. Projected two-electron momentum distribution $P(k_{1,z}, k_{2,z})$ for (a) the ground state of helium, (b) the ground state wave function boosted by the one-body boost operator B_{1B} with a momentum transfer $\Delta p_e = 1.0$ a.u., (c) boosted by the collective boost operator B_c (Eq. 4) with identical Δp_e (see text).

where t^{el}_{nuc} is the transition amplitude for elastic nuclear scattering with momentum transfer $\Delta\vec{p}_{nuc} = \vec{k}_f - \vec{k}_i$ and $t^{e}_{i,f}$ is the matrix element of the collective boost operator

$$t^{e}_{i,f}(\Delta\vec{p}_e) = \langle\Psi_f|\exp[i\Delta\vec{p}_e\cdot(\vec{r}_1+\vec{r}_2)]|\Psi_i\rangle \tag{2}$$

with

$$\Delta\vec{p}_e = -\frac{\Delta\vec{p}_{nuc}}{M_\alpha+2} \tag{3}$$

and M_α the mass of the α particle in atomic units. Taylor expansion of the collective boost operator

$$B_c(\Delta\vec{p}_e) = \exp[i\Delta\vec{p}_e\cdot(\vec{r}_1+\vec{r}_2)] \tag{4}$$

$$\approx 1 + i\Delta\vec{p}_e\cdot(\vec{r}_1+\vec{r}_2) - \frac{1}{2}[\Delta\vec{p}_e\cdot(\vec{r}_1+\vec{r}_2)]^2 \tag{5}$$

shows that while the electronic transition matrix element, to first order in $\Delta\vec{p}_e$, is equivalent to that of the one-body operator from photoabsorption or the Bethe-Born limit of soft charged-particle collisions, all higher-order terms represent a true many-body transition structurally different from photon or charged-particle interactions. Application of the collective boost to the exact helium ground state (Fig. 1) leads to a correlated displacement of the projected two-electron momentum distribution unlike the one-body boost operator, $B_{1B}(\Delta\vec{p}_e) = \sum_{i=1}^{N}\exp(i\Delta\vec{p}_e\cdot\vec{r}_i)$ governing, for example, Compton scattering or charged particle impact on an N-electron atom. This property plays a key role in accessing states blocked by parity or propensity rules.

Differential cross sections for electronic inelastic processes accompanied by quasi-elastic neutron-alpha particle scattering are given by

$$\frac{\mathrm{d}\sigma_{i\to f}}{\mathrm{d}\Omega}(\Delta\vec{p}_{nuc}) = \frac{k_f}{k_i}\frac{\mathrm{d}\sigma_{el}}{\mathrm{d}\Omega}(\Delta\vec{p}_{nuc})|t^{e}_{i\to f}(\Delta p_e)|^2 \tag{6}$$

with $k_f = \sqrt{k_i^2 - 2\mu Q_I}$, $Q_I = E^e_f - E^e_i$ the internal excitation energy, and μ the reduced mass of the n-He system.

For the nuclear elastic scattering cross section $\frac{\mathrm{d}\sigma_{el}}{\mathrm{d}\Omega}$ we use the tabulated data from [14]. For the electronic degrees of freedom in helium we perform full ab-initio calculations by solving the six-dimensional time-independent Schrödinger equation (five-dimensional after exploiting cylindrical symmetry) including all interparticle interactions. In our computational approach we employ a close-coupling scheme, in which the angular variables are expanded in coupled spherical harmonics (with total angular momentum up to $L_{\max} = 7$, and individual electron angular momenta up to $l_{\max} = 9$). For the discretization of the radial components we use a finite element discrete variable representation (FEDVR) [15, 16]. The momentum boost operator Eq. (5) is implemented using a short iterative Lanczos algorithm (SIL) [17]. For

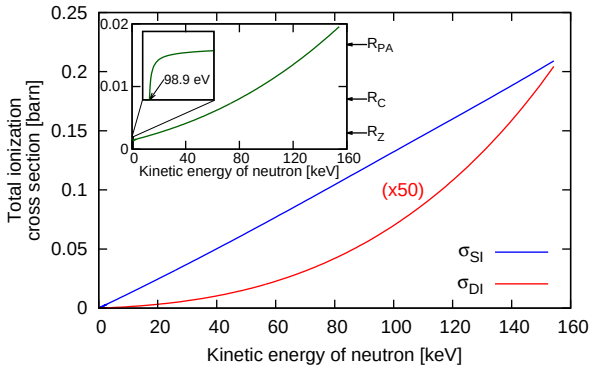

FIG. 2. (Color online) Absolute integrated double (σ_{DI}) and single ionization (σ_{SI}) cross section by neutron impact as a function of the neutron kinetic energy. Inset: Energy dependence of $R_{\mathrm{N}} = \sigma_{\mathrm{DI}}/\sigma_{\mathrm{SI}}$ with magnification of threshold region. The nonrelativistic high-energy limits for photoabsorption R_{PA}, Compton scattering R_{C}, and charged particle impact R_{C} are shown for comparison.

the extraction of transition amplitudes, the direct projection onto final states would be most desirable but unfeasible as exact three-body Coulomb continuum states are not known. We therefore make use of an alternative approach [7, 18], in which the Fourier transform of the boosted wave packet is effectively calculated by solving the inhomogeneous linear system

$$(E-H)|\Psi_{\mathrm{sc}}(E)\rangle = B_c(\Delta\vec{p}_e)|\Psi_i\rangle, \tag{7}$$

where $\Psi_{\mathrm{sc}}(E)$ is the scattered wave function in the (time-independent) energy domain. Outgoing boundary conditions are enforced by an exterior complex scaling (ECS) transformation for each of the radial coordinates. For the calculations presented in this Letter we chose an exterior scaling radius of 120 a.u. and an overall box size of up to 180 a.u.. The ejected single and double ionization amplitudes can then be extracted from the scattering amplitude by means of a surface integral within the non-scaled part of the grid [18].

The most frequently studied quantity in double ionization of helium, a paradigm for studying the role of electron correlation, is the ratio of double to single ionization R. This ratio has been probed for both charged particle impact and photon impact over a wide range of energies, both experimentally and theoretically [20]. For photon impact, photoabsorption as well as Compton scattering have been studied [19, 21–26]. The corresponding ratio R_{N} for neutron impact ionization is obtained as a function of the kinetic energy of the incident neutron by integrating Eq. (6) over all accessible final states in the $\Delta\varepsilon$-Δp_e plane (inset Fig. 2). With increasing neutron energy the ratio R_{N} increases polynomially ($\propto a_1E_{\mathrm{N}} + a_2E_{\mathrm{N}}^2 + \cdots$) with the neutron energy and eventually surpasses the well known (non-relativistic) high-energy limits for photoabsorption (1.66%) [21–24],

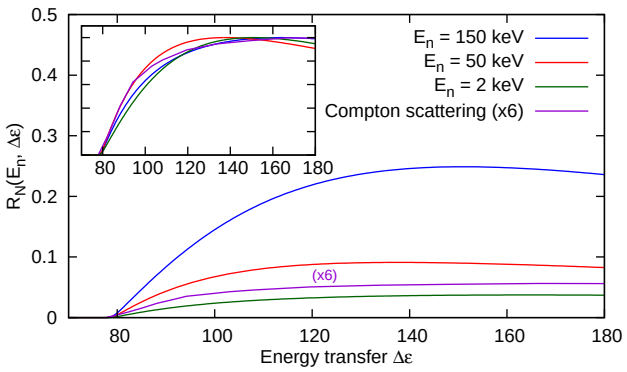

FIG. 3. (Color online) Ratio of double to single ionization for neutron-impact ionization $R_{\rm N}(\Delta\varepsilon)$ as a function of energy transfer $\Delta\varepsilon$ compared to the corresponding ratio $R_{\rm C}$ for Compton scattering [19] multiplied by a factor 6 for visibility. Inset: The same ratios normalized to their respective maxima.

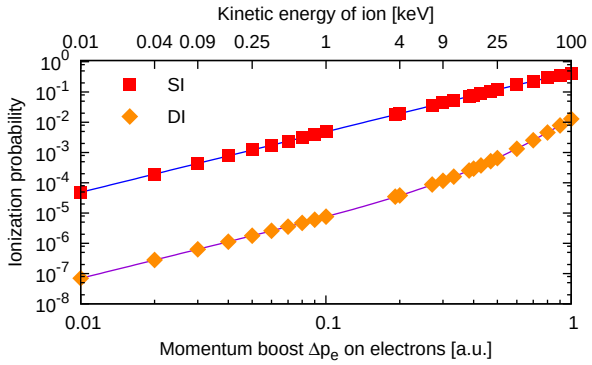

FIG. 4. (Color online) Single (SI) and double ionization (DI) probabilities of helium as a function of the momentum boost Δp_e for the electrons. The corresponding recoil energy of the kicked helium nucleus is given on the upper abscissa.

Compton scattering (0.8%) [19, 25, 26] and charged-particle impact (0.26%) [20, 27]. The reason is that for large energy transfers the helium nucleus suddenly "disappears" from the electronic charge cloud resulting in a high probability for double ionization.

Compton scattering, involving a high energy neutral projectile, is expected to bear closest resemblance to the present case of neutrons. The ratio $R_{\rm N}(\Delta\varepsilon)$, differential in energy transfer $\Delta\varepsilon$ to the electronic system, indeed, qualitatively resembles the calculated $R_{\rm C}(\Delta\varepsilon)$ for Compton scattering near threshold (inset Fig. 3). Its absolute magnitude is, however, strongly enhanced by factors up to 25 depending on the kinetic energy of the incident neutron (Fig. 3). This difference is expected, as for neutrons the collective boost rather than the one-body boost controls the transition and, moreover, different regions in the energy transfer ($\Delta\varepsilon$) - momentum transfer (Δp_e) plane are sampled. The most dramatic difference (Fig. 4) occurs for large momentum transfers due to the non-linear dependence of the boost operator on Δp_e. In the limit $\Delta p_e \to \infty$, or more precisely when the momentum transfer is large compared to the width of the momentum distribution of the initial state, $\Delta p_e \gg \langle p_e^2\rangle^{\frac{1}{2}}$ (i.e., the Compton profile), the ratio diverges, as the strongly displaced momentum distribution (Fig. 1) will effectively cease to overlap with bound states and double ionization dominates.

A more sensitive probe of the momentum shift of the two-electron momentum distribution by the collective boost is the energy spectrum of the ejected electrons in single and double ionization (Fig. 5). The impulsive momentum transfer leads to a broad-band excitation (the upper cut-off due to the finite nuclear collision time $\sim 1/t_{coll}$ lies well beyond the spectral range shown in Fig. 5) resulting in a large number of doubly excited resonances embedded in the single ionization continuum. A zoom into the electron energy spectrum just below the $n = 2$ threshold [Fig. 5(c)] shows the multitude of Beutler-Fano resonances of different symmetries. Note that doubly excited states are not properly identified by the usual independent-particle labels, but require collective quantum numbers (cf. [1] and references therein). However, for brevity, we use the traditional but imprecise labels $(nl\,n'l')$ to describe the first few doubly excited states. The background from direct single ionization into the continuum is only strong in the channel with $^1P^{\rm o}$ final symmetry, while it is suppressed in the other channels. This is a clear signature of the different dominant terms in the transition operator for different symmetries: in $^1P^{\rm o}$, the first-order (one-body) part dominates, which couples efficiently to the single continuum, but only weakly to doubly excited states. In $^1S^{\rm e}$ and $^1D^{\rm e}$, the dominant part of the boost operator is the second-order two-body term. The latter couples the initial ground state more efficiently to the quasi-bound doubly excited states than to the single ionization continuum. This is best seen in the $(2p)^2$ (both in the $^1S^e$ as well as in the $^1D^e$ channel) and $(2p3p)$ doubly excited states which feature the largest cross section. By contrast, these transitions are strongly forbidden in photoabsorption driven by the dipole operator (first term in Eq. 5). Exciting those resonances by photons would require a two-photon absorption process triggered by an intense beam with well-tuned frequencies, in reach with free-electron lasers [29, 30]. Even within the dipole-allowed $^1P^{\rm o}$ spectrum neutron-impact ionization leads to a marked modification of the Beutler-Fano resonance profiles [3] compared to photoabsorption [Fig. 5(b),(c)]. The latter is a signature of interference between the first and odd higher order terms in Eq. 5.

It is instructive to compare the neutron-impact induced spectrum with the corresponding spectrum for electron impact [Fig. 5(d), taken from [28]]. While for charged-particle collisions higher multipole transitions become allowed, the propensity for excitation of res-

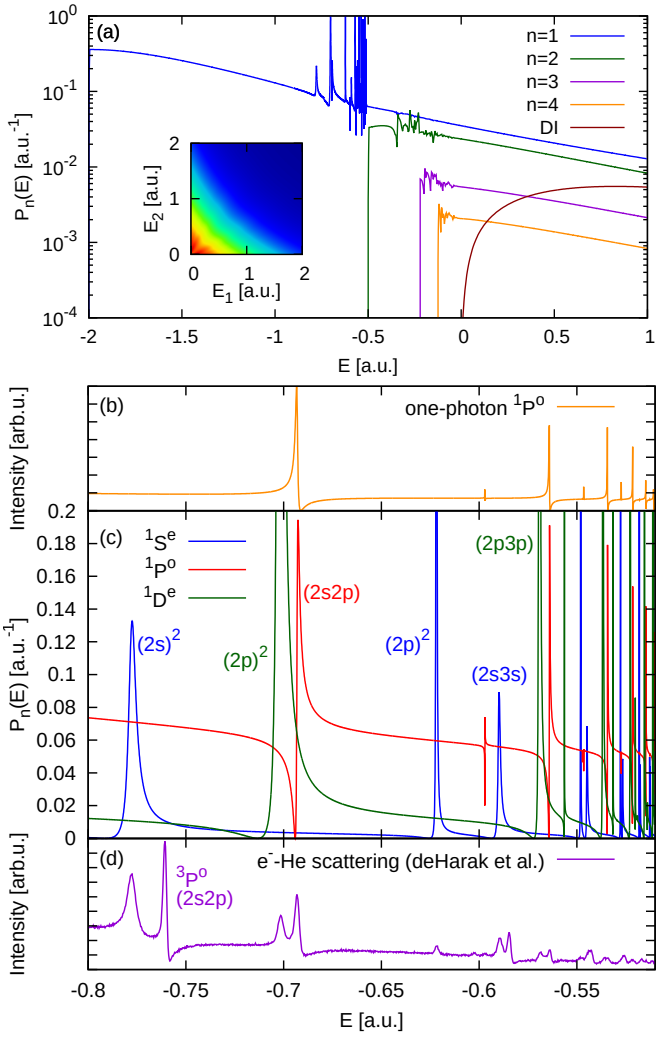

FIG. 5. (Color online) (a) Electron spectrum as a function of final energy for single and double ionization for a kick strength of $\Delta p_e = 1$ a.u.. The energy of the ejected electron in the case of SI is given by $E + \frac{2}{n^2}$ with the remaining ionized helium being excited to state n. In the case of double ionization the probability for ejecting electrons with the sum of the individual electron energies equivalent to E is plotted. The full two-electron energy distribution is plotted in the inset of (a). A close-up of Fano resonances in the $n = 1$ channel for different final symmetries is shown in (c). The first few resonances are labeled by approximate independent-particle configurations. For comparison, the one-photon spectrum (b, calculated) and an ejected electron spectrum (d) from e^--He scattering experiments performed by deHarak *et al.* [28] are shown.

onances of different symmetry are markedly different. Considering, for example, the first two doubly excited resonances in the $^1S^e$ channel, the $(2p)^2$ state is much stronger excited for neutron impact ionization than for electron scattering. This is in contrast to the $(2s)^2$ doubly excited state, which is present in both excitation processes. This difference can be explained by specific electron correlation effects present in these doubly excited states. It has been shown [4] that a major difference between the two states lies in the expectation value of the angle θ_{12} between the two electrons. For the $(2s)^2$ state the electrons are more likely situated opposite to each other whereas in the $(2p)^2$ case they have a tendency to be located on the same side of the nucleus. For the quasi-instantaneous neutron kick it is suggestive that both electrons will be pushed to the same side of the nucleus (Fig. 1) and will thus have significant overlap with this class of resonances. This behavior is less likely for excitation by an incoming electron which interacts with the bound electrons via the long-ranged Coulomb force and gives rise to transition matrix elements containing the one-body boost operator. The strong excitation can thus be directly attributed to the effective many-body nature of the neutron kick. In contrast to neutron impact, the collision with an incoming electron can also access $^3P^o$ states due to spin exchange processes, which can be seen in Fig. 5(d) for the $^3P^o(2s2p)$ state.

We finally turn to the prospects of experimental realization of neutron-impact ionization. The most easily accessible quantity is the ratio $R_{\rm N}$ of double to single ionization. It only involves the integral detection of charge-state selected recoil ions without momentum resolution. $R_{\rm N}$ is well suited to compare different excitation mechanisms (Fig. 2). A more challenging experiment would be the electron spectroscopy of doubly excited resonances (Fig. 5). Here, the momenta of both the ion and the electrons need to be measured in coincidence, which can be accomplished in a reaction microscope-like COLTRIMS setup [31]. Note that the detection of the quasi-elastically scattered neutron is not needed in either case.

In conclusion, we have shown that neutron-impact ionization could serve as a novel tool to probe correlated electronic dynamics in many-body electron systems, specifically in helium. Key is the true many-body nature of the correlated boost operator which allows transitions that are either strictly forbidden or strongly suppressed in either photoabsorption or charged-particle excitation. Doubly excited resonances become prominent that are otherwise only barely visible. The ratio of double to single ionization by neutrons, $R_{\rm N}$, is another benchmark for the underlying differences of the ionization process. The predicted ratios significantly differ from those for photoabsorption, Compton scattering, and charged-particle collisions. With the availability of high-intensity neutron sources, the observation of these processes under well-characterized single-collision conditions may come into reach.

We thank B. deHarak for providing us with the data of the e^--He scattering measurements. S.N. and J.B. acknowledge support by the FWF-Austria, SFB-041 VICOM and P23359-N16. J.F. acknowledges support from the NSF through a grant to ITAMP. M.L. acknowledges funding by the Vienna Science and Technology Fund

(WWTF) through project MA09-030. The computational results have been achieved using the Vienna Scientific Cluster and NSF TeraGrid/XSEDE resources provided by NICS and TACC under grant TG-PHY090031.

* matthias.liertzer@tuwien.ac.at

[1] G. Tanner, K. Richter, and J. M. Rost, Rev. Mod. Phys **72**, 497 (2000).

[2] G. H. Wannier, Phys. Rev. **90**, 817 (1953).

[3] H. Beutler, Z. Phys. A **93**, 177 (1935); U. Fano, Nuovo Cimento (1924-1942) **12**, 154 (1935); Phys. Rev. **124**, 1866 (1961).

[4] O. Sinanoğlu and D. R. Herrick, J. Chem. Phys. **62**, 886 (1975).

[5] S. L. Carter and H. P. Kelly, Phys. Rev. A **24**, 170 (1981).

[6] U. Fano and A. R. P. Rau, *Atomic Collisions and Spectra* (Academic Press Inc, 1986).

[7] C. W. McCurdy, M. Baertschy, and T. N. Rescigno, J. Phys. B **37**, R137 (2004).

[8] A. S. Kheifets and I. Bray, Phys. Rev. A **54**, R995 (1996); J. S. Parker, E. S. Smyth, and K. T. Taylor, J. Phys. B **31**, L571 (1998); E. Foumouo, P. Antoine, B. Piraux, L. Malegat, H. Bachau, and R. Shakeshaft, J. Phys. B **41**, 051001 (2008).

[9] J. Berakdar, J. Phys. B **35**, L31 (2002).

[10] V. Sears, Physics Reports **141**, 281 (1986).

[11] M. Hentschel, R. Kienberger, C. Spielmann, G. A. Reider, N. Milosevic, T. Brabec, P. Corkum, U. Heinzmann, M. Drescher, and F. Krausz, Nature **414**, 509 (2001).

[12] M. Drescher, M. Hentschel, R. Kienberger, G. Tempea, C. Spielmann, G. A. Reider, P. B. Corkum, and F. Krausz, Science **291**, 1923 (2001).

[13] F. Krausz and M. Ivanov, Rev. Mod. Phys **81**, 163 (2009).

[14] The angular dependent differential cross section has been obtained from the sigma database at the National Nuclear Database Center (NNDC).

[15] J. Feist, S. Nagele, R. Pazourek, E. Persson, B. I. Schneider, L. A. Collins, and J. Burgdörfer, Phys. Rev. A **77**, 043420 (2008).

[16] J. Feist, S. Nagele, R. Pazourek, E. Persson, B. I. Schneider, L. A. Collins, and J. Burgdörfer, Phys. Rev. Lett. **103**, 063002 (2009).

[17] T. J. Park and J. C. Light, J. Chem. Phys. **85**, 5870 (1986).

[18] A. Palacios, C. W. McCurdy, and T. N. Rescigno, Phys. Rev. A **76**, 043420 (2007).

[19] J. Burgdörfer, Y. Qiu, J. Wang, and J. H. McGuire, AIP Conference Proceedings **389**, 475 (1997).

[20] For a review, see J. H. McGuire, N. Berrah, R. J. Bartlett, J. A. R. Samson, J. A. Tanis, C. L. Cocke, and A. S. Schlachter, J. Phys. B **28**, 913 (1995).

[21] F. W. Byron and C. J. Joachain, Phys. Rev. **164**, 1 (1967).

[22] T. Åberg, Phys. Rev. A **2**, 1726 (1970).

[23] A. Dalgarno and H. R. Sadeghpour, Phys. Rev. A **46**, R3591 (1992).

[24] L. R. Andersson and J. Burgdörfer, Phys. Rev. Lett. **71**, 50 (1993).

[25] L. R. Andersson and J. Burgdörfer, Phys. Rev. A **50**, R2810 (1994).

[26] T. Surić, K. Pisk, B. A. Logan, and R. H. Pratt, Phys. Rev. Lett. **73**, 790 (1994).

[27] L. H. Andersen, P. Hvelplund, H. Knudsen, S. P. Moller, A. H. Sorensen, K. Elsener, K. G. Rensfelt, and E. Uggerhoj, Phys. Rev. A **36**, 3612 (1987).

[28] The spectrum, originally published in B. A. deHarak, J. G. Childers, and N. L. S. Martin, Phys. Rev. A **74**, 032714 (2006), was taken at an angle of 120° with respect to a 75 eV incident electron beam.

[29] R. Moshammer, Y. H. Jiang, L. Foucar, A. Rudenko, T. Ergler, C. D. Schröter, S. Lüdemann, K. Zrost, D. Fischer, J. Titze, T. Jahnke, M. Schöffler, T. Weber, R. Dörner, T. J. M. Zouros, A. Dorn, T. Ferger, K. U. Kühnel, S. Düsterer, R. Treusch, P. Radcliffe, E. Plönjes, and J. Ullrich, Phys. Rev. Lett. **98**, 203001 (2007).

[30] A. A. Sorokin, M. Wellhofer, S. V. Bobashev, K. Tiedtke, and M. Richter, Phys. Rev. A **75**, 051402(R) (2007).

[31] J. Ullrich, R. Moshammer, A. Dorn, R. Dörner, L. P. H. Schmidt, and H. Schmidt-Böcking, Rep. Prog. Phys. **66**, 1463 (2003).